X-611-69-427

PREPRINT

NASA TM X-63691

CHEMICAL COMPOSITION OF RELATIVISTIC COSMIC RAYS DETECTED ABOVE THE ATMOSPHERE

SEPTEMBER 1969

GSFC

GODDARD SPACE FLIGHT CENTER

GREENBELT, MARYLAND

Chemical Composition of Relativistic Cosmic Rays Detected Above the Atmosphere

N. Durgaprasad*
C. E. Fichtel
D. E. Guss+
D. V. Reames

NASA/Goddard Space Flight Center, Greenbelt, Md.

F. W. O'Dell
M. M. Shapiro
R. Silberberg
B. Stiller
C. H. Tsao

Lab. for Cosmic-Ray Physics, Naval Research Laboratory
Washington, D. C.

*National Academy of Sciences-National Research Council Resident Research Associate while at Goddard Space Flight Center. Present address: Tata Institute of Fundamental Research, Bombay, India.

+Deceased.

Chemical Composition of Relativistic Cosmic Rays Detected Above the Atmosphere

N. DURGAPRASAD*, C. E. FICHTEL, D. E. GUSS+, D. V. REAMES
NASA/Goddard Space Flight Center, Greenbelt, Md.

F. W. O"DELL, M. M. SHAPIRO, R. SILBERBERG, B. STILLER, C. H. TSAO
Naval Research Laboratory, Washington, D. C.

ABSTRACT

Final results on the first satellite experiment on abundances of cosmic-ray nuclei having a mean energy of several GeV per nucleon are presented. A nuclear emulsion detector, exposed on Gemini XI in a near-equatorial orbit ranging between geographic latitudes $\pm 29°$, collected 619 high-quality tracks above the earth's atmosphere. Time resolution (within about 5 minutes) was provided by movement of a lower emulsion stack relative to an upper one. The detector was covered by only 0.07 g/cm^2 of aluminum, and was favorably oriented for 18 hours. The results on abundances, requiring no correction for secondary production in the atmosphere are characterized by: (a) a pronounced odd-even effect, with low abundances for elements of atomic number 7, 9, 11 and 13, compared to those of neighboring elements with even Z; (b) approximately equal fluxes of neon, magnesium and silicon, each being about one-fourth that of oxygen; and (c) an abundance gap in the region $15 \leq Z \leq 19$. The observed ratios of Be + B, $10 \leq Z \leq 19$, and $Z \geq 20$ to the medium group, $6 \leq Z \leq 9$, provide no evidence for significant variation of composition with rigidity between 3.5 GV and 30 GV. A primordial composition--prior to interactions of the cosmic rays with the interstellar medium--is calculated. This source composition is compared with "universal" and solar abundances.

*National Academy of Sciences-National Research Council Resident Research Associate while at Goddard Space Flight Center. Present address: Tata Institute of Fundamental Research, Bombay, India.
+Deceased

I. INTRODUCTION

A knowledge of the composition of the heavy nuclei in the galactic cosmic radiation is useful in shedding light on the nature of cosmic ray sources, on the interactions of cosmic rays in the tenuous interstellar gas, and on the amount of material traversed before escaping the galaxy. In previous work at high energies ($\geq$ 1 GeV/nucleon) the experiments were carried out with balloons, but even in good high-altitude flights, one had to correct through about 0.1 or 0.2 mean free paths of atmosphere to deduce the original composition. These corrections (as well as the ascent correction) involve uncertainties due to insufficient knowledge of fragmentation cross sections in nucleus-nucleus collisions. While the correction is not serious for elements that are abundant in cosmic ray sources (such as C, O, Ne, Mg, Si, and Fe), it affects the data of the abundances of other elements to an appreciable degree. Also, most radioactive isotopes produced in collisions with air nuclei will be recorded as such rather than as the final decay product, e.g., C^{11} will be recorded as carbon rather than boron, whereas for collisions with interstellar gas the opposite is the case. Hence, an experiment above the atmosphere can yield more accurate information on the abundances of Be, B, N, and higher-charged odd-Z elements, particularly if the area-time factor for the collection of tracks is adequate.

The Gemini XI emulsion experiment is the first flight above the atmosphere and on the exterior of a spacecraft, with a sufficient time-area factor to explore some of the above-discussed relative

abundances of elements at energies $\geq$ 1 GeV/nucleon, and to verify previous assumptions regarding partial fragmentation cross sections in air. The orientation of the spacecraft, and the location of apogees in the high-altitude orbits were optimized to reduce the detrimental effects of the slow Van Allen-belt protons on the scan for the heavy primary nuclei. Even under these circumstances, detection of the lightly ionizing lithium nuclei was prohibitively difficult, and the efficiency for beryllium was low. Time resolution for entrance of tracks was provided in order to eliminate particles arriving at times of poor spacecraft orientation, and to provide crude energy estimates from values of cut-off rigidities.

II. EXPERIMENT

The Gemini missions offered one of the first opportunities to study the cosmic radiation above the earth's atmosphere using the nuclear emulsion technique. Previous space experiments were placed inside spacecraft where the amount of intervening matter of several g/cm^2 was much more than is present on balloon flights.[1,2] However, there were other constraints, including size, weight, a variable orientation, limited exposure time, and the need for temperature control. Since there were periods of the flight when the apparatus might be pointing toward the earth and a period in the latter portion of the flight when the detector would be inside the spacecraft, it was necessary to know when a given particle entered. There are several ways of achieving time resolution with nuclear emulsion despite the fact that it is a continuously integrating detector.[3] The method

used in this experiment was the slow movement of one block of emulsions with respect to another; this procedure will be described in detail later in this section. The other principal problem was recovery of the emulsion from its external location after exposure. To accomplish this, the experimental package was retrieved by astronaut Richard F. Gordon, Jr., during the period that he was outside the spacecraft, and was placed inside the cabin where it remained for the rest of the flight. In the following paragraphs, a general description of the detector system will be given, together with a discussion of the methods used to solve the problems which had to be cvercome.

The entire experiment was contained in a metal box approximately 3.0 inches by 8.5 inches laterally and 6.0 inches deep; the shape was determined primarily by the size and shape of the available space. The upper surface of the box had a 0.010-inch aluminum window so that there would be a minimum amount of material between the emulsions and ambient radiation consistent with a light-tight pressure seal, which also kept the nuclear emulsions at a known humidity level. The upper stack of nuclear emulsions was 1/2" deep and consisted of 91 Ilford K.5 emulsions, all but two of which were 600 microns thick. The remaining two were 200 microns thick. K.5 emulsions were selected so that minimum ionizing tracks left by particles coming from interactions could be seen. Below this shallow stack was a 2.25-inch deep stack which was two inches shorter than the upper one and could move with respect to it when driven by a motor. The position of these two sets of nuclear emulsions is shown in Fig. 1. In the lower stack, with the exception of three 200μ

plates, all nuclear emulsions were 600μ thick; however, in this case, they were of various sensitivities to aid in the charge identification of the particles. In general, the stack was assembled in a repeating sequence of emulsion types, which was: K.2, K.5, K.2, G.0, K.2.

The lower stack had a total travel length of 2.0 inches. To conserve power, it was moved by a motor in increments of 0.001 inch rather than continuously. This stepped motion was of no disadvantage to the experiment because 0.001 inch is less than the minimum resolvable displacement. When the experiment was in its normal mode of operation, the lower stack was advanced one every 60 seconds, so that the total 2.0 inch travel could be accomplished in 33 1/3 hours. A backup mode, which was not used in flight, allowed the stack to be advanced in 0.008 inch increments at times at least 10 seconds apart, by activating a switch in the astronaut's cabin. The time of each advancement of the stack was recorded, stored on tape, and later transmitted to the ground data acquisition system. A detailed description of the mechanical system is given elsewhere.[4]

Several unique problems arose in connection with the experiment. One was the need to keep the nuclear emulsions within tolerable temperature limits. This was accomplished by circulating the coolant of the spacecraft temperature control system through plates making up the walls of the external well in which the nuclear emulsion experiment was placed and by covering the upper surface of the metal box with a thin thermally reflective coating. There was the further problem of high temperature during launch, which was solved by placing a thermal shield over the

nuclear emulsion detector system during the launch phase. This cover was blown off after orbit was achieved.

In addition to the considerations mentioned earlier concerning the thin window above the emulsion, the possibility of puncture by micrometeorites was also considered. For the area and thickness used and a two-day exposure in space, the probability of a puncture was of the order of 3×10^{-6} or less.[5-8]

The first opportunity to conduct the experiment was provided on the flight of Gemini VIII, launched in March, 1966. Malfunction of a spacecraft component led to an emergency requiring premature termination of this mission, and the experimental package was lost. The first successful exposure of the detector to the cosmic radiation was provided on the Gemini XI mission.

At approximately 55 hours prior to launch, the package was installed in its temperature-controlled well aboard the spacecraft and telemetry checks were made to verify correct installation. The spacecraft was launched at 08:42:23 E.D.T. (00:00:00 G.E.T., Ground Elapsed Time) on August 12, 1966, with astronauts Charles Conrad and Richard Gordon. Movement of the lower stack of emulsion was initiated by an astronaut at 01:42:29 G.E.T. During the period of data collection, telemetered information confirmed that the equipment was functioning and that its temperature was being properly controlled.

The spacecraft was oriented so that the emulsion layers were nearly vertical for as much of the time as would be commensurate with other operational requirements during the data collection period. In addition,

whenever the spacecraft passed through the South Atlantic Anomaly region, the astronauts oriented it with its blunt end forward, thereby placing the detector window nearly perpendicular to the local magnetic field line in order to minimize the background effect produced by tracks of protons mirroring along magnetic field lines. At 24:05:50 G.E.T. the package was removed from its external well and stowed in the command module of the spacecraft. During the remaining two days of the mission, the package was partially shielded from Van Allen particles by the spacecraft. Tracks made by heavy primary nuclei arriving during this period could be eliminated from the analysis because they would produce a large peak at the same displacement between their positions in the upper and lower nuclear emulsion stacks. After reentry and recovery of the spacecraft, the package was removed from the spacecraft and flown to Patrick Air Force Base, Florida, where it was returned to project scientists.

Trial processings were carried out on selected exposed emulsions in order to determine an optimum procedure for minimizing the obscuration produced by background tracks. The stacks were then processed by a technique involving temperature-cycling and a liquid warm stage.

III. DATA REDUCTION

A. Scanning and Track Matching

The stack was equally divided between the NRL and GSFC groups for purposes of scanning and data reduction. Although there were some differences in the techniques employed by the two laboratories, the general procedures used were as follows:

The K.2 and K.5 pellicles in the lower stack were scanned along a line 5 mm below the upper edge of the stack for particle tracks satisfying the following geometrical and ionization restrictions:

(1) Projected track length per plate $\geq$ 2 mm.

(2) Projected angle with the normal to the collection edge $\leq 60°$.

(3) Ionization $\geq$ 9 times minimum.

(With the latter criterion, a large fraction of the low energy protons could be excluded from the initial scan.) Coordinates at 3 or more points along each track that did not end in the scan plate were recorded using three-coordinate digitized microscopes. Singly charged background tracks included in this collection were eliminated on the basis of multiple scattering measurements and track following through the lower stack. The remaining tracks whose ionization and path length in emulsion indicated that they were made by heavy nuclei were projected upward to a scan line 4 mm above the lower edge of the upper stack. The predicted locations along this line were used as a guide to locate the matching track segments in the upper stack.

The displacement of a track in the lower stack from the position it would have had if the stack had not moved is a measure of the time of arrival of the particle which made the track. Fig. 2 is a plot of the distribution of the measured tracks as a function of displacement and hence ground elapsed time. The small peak at the left shows the accumulation of tracks prior to actuation of stack motion. The more pronounced peak at the right represents the tracks accumulated after

cessation of stack motion. The shape of this peak was used to evaluate the uncertainty in arrival time of a particle. This uncertainty is ± 5 minutes which is equivalent to 125 microns of displacement.

Tracks accumulated between the peaks in Fig. 2 were followed for their entire length in the emulsion; those which interacted above the scan line in the lower plate were rejected. Interactions below the scan line were examined and in all cases were consistent with fragmentation of a downward-moving primary.

Slightly over 20% of the plates were rescanned to determine scanning efficiencies. Since all heavy nuclei recorded in the rescan could be used for this purpose, independent of entry time, the total number of tracks involved was 397 or about 64% as large as the final data sample. The overall scanning efficiency was found to be 95%. The efficiency was a function of particle charge and varied from 77% for beryllium nuclei to 98% for heavy nuclei (see Table I-a).

B. Charge Analysis

Particle charge estimates were based on delta-ray measurements in K.5 emulsion and grain density measurements in the less sensitive K.2 and G.5 emulsions. Two or more independent charge determinations were made on most of the tracks. The final charge assigned to each particle was a suitably weighted average of the values deduced in the different emulsion types. The observed charge distribution is shown in Fig. 3. The plot includes only those tracks meeting the arrival direction criteria explained in section C below.

The low abundances of the elements F, Na, and Al make their resolution from neighboring elements difficult. In addition, the experimental errors associated with the charge measurements in this region do not permit unambiguous resolution of individual charges. Therefore, the abundances of F, Na, and Al are shown as upper limits in Table I and Figure 4; their actual abundances are certainly smaller than these limits.

C. Correction for Spacecraft Orientation

Since the spacecraft was not always oriented so that the nuclear emulsion stack was facing upward, it was necessary to determine the arrival direction of each particle in the earth's coordinate system from a knowledge of its arrival time, its angle in the emulsion, the spacecraft orientation, and the spacecraft position. The method by which these directions were determined is given in the Appendix. To insure that the track being analyzed was a primary and not one which had passed through a portion of the atmosphere, tracks were accepted for analysis only if the arrival direction of the corresponding particle was within 73° of the local vertical. In practice, the uncertainty in arrival time introduced an uncertainty in arrival direction. Using the distribution of the tracks in the final peak of Fig. 2 as the probability distribution for arrival time about the measured one, the probability that a given track arrived within 73° of the vertical could be calculated. All tracks with a probability of less than 0.7 of having arrived within 73° of the vertical were rejected. Of the 619 tracks in the final

analysis, 132 had probabilities as defined above between 0.7 and 0.999; the rest had probilities which were within 0.1% of 1.000.

D. Cutoff Rigidity

In order to look for possible variations in the composition with energy and to provide a test of the approach just described, the following procedure was used. The vertical rigidity[9] cutoff is calculated from the relation

$$R_v = 15.96/L^{2.005} \tag{1}$$

where L is defined in the B-L coordinate system[10] and is calculated using a program developed by Hendricks and Cain.[11] The cutoff as a function of the azimuthal and zenith angles is then calculated using the angular dependence of the cutoff valid for a dipole and normalizing to the vertical cutoff rigidity discussed above. The cutoff rigidity is then

$$R = \frac{15.96}{L^{2.005}} \left\{ \frac{2}{1 + (1 - L^{-3/2} \sin\theta \sin\omega')^{1/2}} \right\}^2 \tag{2}$$

where ω' is the azimuthal angle in the horizontal plane expressed in magnetic coordinates and θ is the zenith angle. (The $\cos^3\lambda'$ normally appearing in the expression for the angular dependence of the dipole threshold rigidity was replaced by $L^{-3/2}$ to be consistent with the vertical rigidity cutoff calculation.)

To calculate the expected number of particles as a function of cutoff rigidity, the solid angle of observation was divided into 48 intervals, and the cutoff rigidity was calculated for each interval for every two minutes during the exposure period. The previously-measured[12-15]

cosmic-ray flux above each calculated cutoff rigidity was then spread over the neighboring time intervals in accordance with the time-of-arrival error distribution. The flux thus accumulated in a given solid-angle, time-interval bin was assigned the cutoff rigidity appropriate to that bin and an integration (summation) over time and solid angle was performed to obtain the number of tracks expected as a function of cutoff rigidity. This distribution was then compared with the cutoff rigidity distribution obtained from the observed tracks using the most probable arrival time to define the cutoff rigidity of each track. A test of the goodness of fit gave a Chi-square value divided by the number of degrees of freedom (five) of 1.33. If $\cos^3\lambda'$ is used in Eq. (2) instead of $L^{-3/2}$, the Chi-square value divided by the number of degrees of freedom becomes 2.85, and, if a dipole approximation is used for R_V as well, this parameter becomes 9.50.

IV. RESULTS & DISCUSSION

A. Charge Composition

The relative charge composition obtained in this work is shown in Fig. 4. The plotted values have been corrected for scanning efficiency and for fragmentation loss in the emulsion above the scan line. (See Table I-a.) The maximum fragmentation correction amounts to 11% for the ratio of nuclei having $Z \geq 20$ to oxygen. The final sample excluded particles that had interacted above the scan line. Hence, in correcting for collision losses in emulsion, it was unnecessary to employ fragmentation parameters, which are rather uncertain; only the relatively well-known absorption mean free paths in emulsion were needed. Also obviated

were the uncertain corrections for secondary production in air that are required in balloon flights.

Errors shown in Fig. 4 reflect errors in the determination of the scanning efficiency as well as statistical errors. The results shown are strikingly similar to other measurements of comparable accuracy above the atmosphere,[16-21] even though the latter measurements are at much lower energy. Taken together with recent measurements at balloon altitudes[22-27] at various energies, it is apparent that any variation in the composition with energy is not large.

Since it is possible to assign a cutoff rigidity to each particle based upon its arrival time and direction, it is also possible to examine the composition as a function of cutoff rigidity in the high rigidity region studied in this experiment. For this purpose we have divided the data into cutoff rigidity intervals as shown in Table II. The error in the cutoff rigidity assigned to a particle is typically 15% and is due primarily to uncertainties in arrival time.

Although the statistical weight of the results is limited, it is clear from Table II that the results are consistent with no variation in the composition over the region of observation from 3.5 BV to about 30 BV.

B. Source Composition

The galactic cosmic rays provide us with information related to the composition of their source region, provided their history can be interpreted in a meaningful way. It is generally assumed that the Li, Be, and B nuclei observed in the cosmic radiation are fragments of heavier nuclei which have had nuclear interactions with interstellar

matter. This assumption is based on the fact that the light nuclei are very rare in the universe because they are rapidly destroyed at the high temperatures of stellar interiors. The abundance of light nuclei can then be used to estimate the amount of material traversed by the cosmic radiation in transit from source to earth. The relative abundances of the nuclei at the source can be calculated from this estimate and their observed relative abundances. The method of calculating the source abundances, including the effects of energy loss and fragmentation, is discussed in detail by Beck and Yiou[28] and by Shapiro et al.[29] and the discussion will not be repeated here. In a recent paper by Fichtel and Reames,[30] several different path length distributions were discussed, and it was shown that the deduced source features to be considered here at high energies are not markedly different from those deduced by assuming a single potential path length. Fe is exceptional in this respect, but in the present work it is treated as part of the group $20 \leq Z \leq 28$. Therefore, the treatment here will be limited to consideration of a single path length which is calculated on the assumption of a negligible amount of Be and B at the source.

It is generally assumed that in high-energy nuclear interactions, the daughter particles very nearly retain the original velocity of the parent, hence the results of the calculations are generally in terms of the same energy/nucleon interval. In order to compare the experimental data obtained here with the calculations, the ratios must be converted from the same rigidity interval to the same energy-nucleon interval. Results of this conversion are shown in Table I-b.

Extrapolating the experimental results back to the source in the manner described above, using the fragmentation parameters summarized by Fichtel and Reames[30] and Shapiro and Silberberg[31] and updated to include the results of Yiou,[32] leads to the source composition shown in the second column of Table III. In this analysis it was found that an average path length of 3.9 ± 0.6 g/cm^2 was needed if there were to be no Be and B at the source.

After extrapolation back to the cosmic-ray source, the cosmic ray abundances are remarkably different from the solar[33-38] or universal[39] abundances, as has been noted previously. Besides the relative richness of the heavier nuclei, there are several other interesting features. Carbon is more abundant relative to oxygen than it is in the universe or the sun. As noted previously,[20,40] nitrogen is relatively scarce in the source region.

It is generally thought that the chemical composition of the cosmic rays reflects that of their source, since most acceleration mechanisms would predict no preferential acceleration of heavier nuclei. It is difficult to conceive of a reasonable acceleration mechanism which would, on the one hand, enhance the heavier nuclei relative to oxygen, while on the other, enhancing carbon on the other side of the charge spectrum from oxygen and, at the same time, suppressing the nitrogen abundance relative to both carbon and oxygen. Thus, it seems reasonable to consider the cosmic-ray source composition as truly unique. The concept of the distributions of the chemical species reflecting their origin, where they have been independently determined, has

been established for the sun[41-43] in the case of solar energetic particles of the same charge-to-mass ratios. There, the acceleration mechanism may be different, but probably the significant requirements are that the nuclei be stripped and the energy losses be small, as suggested by the similarity in source spectral shapes.

A more extensive treatment of the cosmic-ray source composition, based mainly on balloon-flight data available prior to this experiment, and using an exponential distribution of path lengths, has been given by Shapiro, Silberberg, and Tsao.[44]

ACKNOWLEDGMENTS

We gratefully acknowledge the collaboration of Astronauts Charles Conrad and Richard F. Gordon. The experiment depended upon their talents as astronauts and their skill in conducting an extravehicular activity, in the course of which the apparatus was recovered. Mr. John Webb of NASA-Goddard Space Flight Center ably designed the mechanism for moving the lower stack. Mr. Joseph Lill of NASA-Manned Spacecraft Center served as expert technical monitor and helped make the experiment possible. Finally, we thank the scanning teams of GSFC and NRL for their devoted efforts in the scanning and measuring done in these emulsions.

APPENDIX

TRANSFORMATION OF NUCLEAR EMULSION COORDINATES TO SPACE COORDINATES

The following procedure was used to convert angles in the nuclear emulsions to angles with respect to the earth in both geographic and geomagnetic coordinates.

Spacecraft Coordinates: With respect to the spacecraft axes, the nuclear emulsion detector is pitched -10°, since it is on the sloping portion of the Gemini service module, and has a roll of +27.5°; i.e., when the spacecraft is defined as being vertical the nuclear emulsion stack is rotated 27.5° to the right side, toward the pilot. These two angles are called P_E and R_E, respectively.

The emulsion coordinates X_E, Y_E and Z_E are then related to the spacecraft coordinates X_S, Y_S and Z_S by the following equations:

$$X_S = X_E \cos P_E - Z_E \sin P_E \tag{A1a}$$

$$Y_S = Y_E \cos R_E - X_E \sin P_E \sin R_E - Z_E \cos P_E \sin R_E \tag{A1b}$$

$$Z_S = Y_E \sin R_E + X_E \sin P_E \cos R_E + Z_E \cos P_E \cos R_E \tag{A1c}$$

A unit vector along a track in the nuclear emulsion has the following components:

$$X_E = \sin A \cos D \tag{A2a}$$

$$Y_E = - \sin D \tag{A2b}$$

$$Z = \cos A \cos D \tag{A2c}$$

where A is the azimuthal angle measured in the plane of emulsion and D is the dip angle.

Combining A1 and A2 yields:

$$X_S = \sin A \cos D \cos P_E - \cos D \sin P_E \quad \text{(A3a)}$$

$$Y_S = -\sin D \cos R_E - \sin A \cos D \sin P_E \sin R_E - \cos A \cos D \cos P_E \sin R_E \quad \text{(A3b)}$$

$$Z_S = -\sin D \sin R_E + \sin A \cos D \sin P_E \cos R_E + \cos A \cos D \cos P_E \cos R_E \quad \text{(A3c)}$$

Earth Orbit Coordinates: The earth-orbit coordinates X_0 , Y_0 and Z_0 are related to the spacecraft coordinates X_S , Y_S and Z_S by the following equations:

$$X_0 = X_S \cos P \cos W + Y_S \sin W - Z_S \sin P \cos W \quad \text{(A4a)}$$

$$Y_0 = -X_S(\cos P \sin W \cos R + \sin P \sin R) + Y_S \cos W \cos R + Z_S (\sin P \sin W \cos R - \cos P \sin R) \quad \text{(A4b)}$$

$$Z_0 = +X_S(-\cos P \sin W \sin R + \sin P \cos k) + Y_S \cos W \sin R + Z_S(\sin P \sin W \sin R + \cos P \cos R) \quad \text{(A4c)}$$

where P, W, and R are respectively the pitch, yaw and roll angles sustained by the spacecraft with respect to the earth-orbit coordinates. When P, W, and R are zero, the two coordinate systems coincide. In these coordinates, Z_0 is the vertical direction (pointing up) and X_0 represents the direction of motion of the spacecraft.

Geographic Coordinates: The earth-orbit coordinates are related to the geographic coordinates by the following equations:

$$X_G = X_0 \cos \lambda + Y_0 \sin \lambda \tag{A5a}$$

$$Y_G = X_0 \sin \lambda + Y_0 \cos \lambda \tag{A5b}$$

$$Z_G = Z_0 \tag{A5c}$$

where λ is the geographic latitude of the spacecraft. Since the spacecraft position and its pitch, yaw, and roll are known as a function of time, the orientation of each track with respect to the local coordinates can be determined. Then,

$$\cos \theta = Z_G \tag{A6a}$$

$$\tan \omega = X_G / Y_G$$

where θ is the zenith angle with respect to the local vertical and ω the azimuthal angle measured in the horizontal plane read clockwise from North.

Geomagnetic Coordinates: The conversion to geomagnetic coordinates is given by the following equations:

$$\cos \lambda' \cos \Phi' = \cos \beta \cos \lambda \cos \Phi + \sin \beta \cos \lambda \sin \Phi \tag{A7a}$$

$$\cos \lambda' \sin \Phi' = - \cos \alpha \sin \beta \cos \lambda \cos \Phi + \cos \alpha \cos \beta \cos \lambda \sin \Phi + \sin \alpha \sin \lambda \tag{A7b}$$

$$\sin \lambda' = \sin \alpha \sin \beta \cos \lambda \cos \Phi - \sin \alpha \cos \beta \cos \lambda \sin \Phi + \cos \alpha \sin \lambda$$

where λ, Φ and λ', Φ' are respectively the latitude, longitude in geographic and geomagnetic coordinates. α is the angle between the geographic and magnetic poles; β is that angle between the two reference axes to which the geographic and geomagnetic longitude are referred.

The azimuthal angle ω' in the geomagnetic coordinates is related to that in the geographic coordinates by the following equation:

$$\omega' = \omega + \sin^{-1}\left[\sin\alpha \sin(\Phi - \Phi_0)\right] /\cos\lambda' \qquad \text{(A8)}$$

where Φ_0 is the longitude of the North magnetic pole read in the geographic frame.

REFERENCES

1. H. Yagoda, Can. J. Phys. 34, 122 (1956).
2. K. I. Alekseeva, L. L. Gabunia, G. B. Zhdanov, E. A. Zamchalova, M. I. Tretjakova and M. N. Shecherbakova, J. Phys. Soc. Japan 17, Supplement A-III, 30 (1962).
3. C. E. Fichtel and J. E. Naugle, "Application of Nuclear Emulsions to Space Research, Including Environmental Testing, Recovery Aspects, and Time Resolution", Proc. IV Internatl. Conf. of Korpuscular Photog., 511, Munich (1962).
4. J. B. Webb, NASA-Goddard Space Flight Center Doc. X-723-66-181 (1966).
5. F. L. Whipple, J. Geophys. Res. 68, 4929 (1963).
6. E. C. Hastings, Jr., NASA TM-949 (1964).
7. R. L. O'Neal, Ed., NASA TM X-1123 (1965).
8. C. A. Gurtler and G. W. Grew, Science 161, 462 (1968).
9. D. F. Smart and M. A. Shea, J. Geophys. Res. 72, 3447 (1967).
10. C. E. McIlwain, J. Geophys. Res. 66, 3681 (1961).
11. S. J. Hendricks and J. C. Cain, J. Geophys. Res. 71, 346 (1966).
12. J. F. Ormes and W. R. Webber, Proc. Ninth Internatl. Conf. on Cosmic Rays, Vol. 1, 349 (1965).
13. K. C. Anand, R. R. Daniel, S. A. Stephens, B. Bhowmik, C. S. Krishna, P. K. Aditya, and R. K. Puri, Tata Institute Rpt. TIFRNE 67-9 (1967).
14. F. Foster and B. E. Schrautemeier, Nuovo Cim. 47A, 189 (1967)
15. P. S. Freier and C. J. Waddington, J. Geophys. Res. 73, 4261 (1968).

16. V. K. Balasubrahmanyan, D. E. Hagge, G. H. Ludwig, and F. B. McDonald, J. Geophys. Res. 71, 1771 (1968).

17. G. M. Comstock, C. Y. Fan, and J. A. Simpson, Astrophys. J. 146, 51 (1966).

18. D. V. Reames and C. E. Fichtel, Phys. Rev. 162, 1291 (1967).

19. G. M. Comstock, C. Y. Fan, and J. A. Simpson, Astrophys. J. 155, 609 (1969).

20. D. V. Reames and C. E. Fichtel, Phys. Rev. 149, 991 (1966).

21. D. E. Hagge, V. K. Balasubrahmanyan, and F. B. McDonald, Can. J. Phys. 46, S539 (1968).

22. F. W. O'Dell, M. M. Shapiro, and B. Stiller, Jour. Phys. Soc. Japan 17, Suppl. A-III, 23 (1962).

23. N. Durgaprasad, Proc. Indian Acad. Sci. 62, Sec. A, 330 (1965).

24. K. C. Anand, S. Biswas, P. J. Lavakare, S. Ramadurai, N. Sreenivasan, V. S. Bhatia, V. S. Chohan, and S. D. Pabbi, J. Geophys. Res. 71, 4687 (1966).

25. W. R. Webber, Handbuch der Physik 46-2, 181, Springer-Verlag, Berlin (1967)

26. W. R. Webber and J. F. Ormes, J. Geophys. Res. 72, 5957 (1967).

27. T. T. von Rosenvinge, J. F. Ormes, and W. R. Webber, Astrophysics and Space Science 3, 80 (1969).

28. F. Beck and F. Yiou, Astrophys. Ltrs. 1, 75 (1968).

29. M. M. Shapiro, R. Silberberg, and C. H. Tsao, Bull. Am. Phys. Soc. II, Vol. 14, 596 (1969). Proc. of the XII Plenary Meeting of COSPAR, Prague, Czechslovakia, May 4-24, 1969. Proc. Internatl. Conf. on Cosmic Rays, Budapest, Hungary, 1969.

30. C. E. Fichtel and D. V. Reames, Phys. Rev. 175, 1564 (1968).

31. M. M. Shapiro and R. Silberberg, High Energy Nuclear Reactions in Astrophysics, Chapter 2, p. 37, Ed. B.S.P. Shen (W. A. Benjamin, Inv., New York, 1967).

32. F. Yiou, Ann. Phys. (France) 3, 169 (1968).

33. S. Biswas, C. E. Fichtel, D. E. Guss, and C. J. Waddington, J. Geophys. Res. 68, 3109 (1963).

34. L. Goldberg, E. A. Muller, and L. H. Aller, Astrophys. J., Suppl. 5, 1 (1960).

35. D. Lambert, Nature 215, 43 (1967).

36. D. Lambert, Monthly Notices of Royal Astron. Soc. 138, 143 (1968).

37. D. Lambert and B. Warner, Monthly Notices of Royal Astron. Soc. 138, 181 (1968a).

38. D. Lambert and B. Warner, Monthly Notices of Royal Astron. Soc. 138, 213 (1968b).

39. A.G.W. Cameron, Proceedings of the Paris Symposium on the Origin and Distribution of the Elements, Pergamon Press, 1968.

40. T. T. von Rosenvinge, W. R. Webber, and J. F. Ormes, Astrophys. and Space Science 3, 4 (1969).

41. S. Biswas and C. E. Fichtel, Space. Rev. 4, 709 (1965).

42. N. Durgaprasad, C. E. Fichtel, D. E. Guss, and D. V. Reames, Astrophys. J. 154, 307 (1968).

43. S. Biswas, C. E. Fichtel and D. E. Guss, Phys. Rev. 128, 2756 (1962); J. Geophys. Res. 71, 4071 (1966).

44. M. M. Shapiro, R. Silberberg, and C. H. Tsao, "Relative Abundances of Cosmic Rays at Their Sources," to be published in Hungarica Physica Acta, 1969.

FIGURE CAPTIONS

Fig. 1: Experimental flight package.

Fig. 2: Distribution of arrival times of heavy primary nuclei.

Fig. 3: Charge estimation from combination of various ionization loss measurements.

Fig. 4: Relative charge composition of cosmic-ray nuclei for the same rigidity interval. (Normalized relative to oxygen) The abundances of Ne, Mg and Si shown include minor contributions from the neighboring odd-charge elements.

TABLE I
Charge Composition
(a)

Z	4	5	6	7	8	9	10	11	12	13	14	15-19	≥20
$N_{observed}$+	8	50	178	42	162	≤6	39	≤5	43	≤10	39	15	30
Scan Efficiency	0.77	0.91	0.94	0.94	0.95	0.97	0.98	0.98	0.98	0.98	0.98	0.98	0.98
Absorption Correction	1.169	1.179	1.189	1.200	1.208	1.218	1.226	1.235	1.243	1.251	1.259	1.284	1.346
N_{true}	12.1	64.8	225.2	53.6	206.0	≤7.5	48.8	≤6.3	54.5	≤12.8	50.1	19.7	41.2
N/N_{oxygen}	0.06 ±.03	0.31 ±.05	1.09 ±.08	0.26 ±.04	1.00* ±.08	≤.04	0.24 ±.04	≤.03	0.26 ±.04	≤.06	0.24 ±.04	0.10 ±.03	0.20 ±.04

(b)

$(2\ Z/A)^{1.5}$	1.07	0.91	1	0.95	1		0.98		0.99		1	0.97	0.90
N'/N'_{oxygen}	0.06 ±.03	0.28 ±.05	1.09 ±.08	0.25 ±.04	1.00 ±.08		0.24 ±.04		0.26 ±.04		0.24 ±.04	0.10 ±.03	0.18 ±.04

+See text for explanation of upper limits for certain odd-charge tracks.

*The error in oxygen has not been incorporated into the errors for the ratios

TABLE III

Relative Abundances of Elements (normalized to oxygen)

Cosmic Rays* (Gemini XI)	Cosmic Rays at Source**	"Universe"	Solar Energetic Particles	Sun
Be 0.06 $\pm$0.03	0+	2.9×10^{-8}	< 0.02	$< 10^{-5}$
B 0.28 $\pm$0.05	0+	2.6×10^{-7}	< 0.02	$< 10^{-5}$
C 1.09 $\pm$0.08	0.89	0.57	0.59 $\pm$0.07	0.60 $\pm$0.10
N 0.25 $\pm$0.04	0.03	0.10	0.19 $^{+0.04}_{-0.07}$	0.15 $\pm$0.05
O 1.00 $\pm$0.08	1.00	1.00	1.00	1.00
F $\leq$ 0.04	0+	1.5×10^{-4}	< 0.03	0.001 (?)
Ne 0.24 $\pm$0.04	0.19	0.10	0.13 $\pm$0.02	0.1 (?)
Na $\leq$ 0.03	0	2.7×10^{-3}	?	0.002
Mg 0.26 $\pm$0.04	0.25	0.04	0.042 $\pm$0.011	0.051 $\pm$0.015
Al $\leq$ 0.06	$\leq$ 0.03	3.6×10^{-3}	?	0.002
Si 0.24 $\pm$0.04	0.33	0.04	0.09	0.045
P-K 0.10 $\pm$0.03	0.04	0.03	$\leq$ 0.02	0.04‡
Ca-Ni 0.18 $\pm$0.03	0.24	0.04	0.011 $\pm$0.003	0.01 (?)

*Compared at the same energies-per-nucleon.

**Extrapolated through 4 g/cm^2 to source. The errors associated with the numbers in this column are typically $\approx$ 20 percent. However, nitrogen and the P-K group are uncertain by a factor of $\approx$ 2.

+Assumed

‡Assuming A to be about half as abundant as S, and the abundance of Cl to be small compared to S.

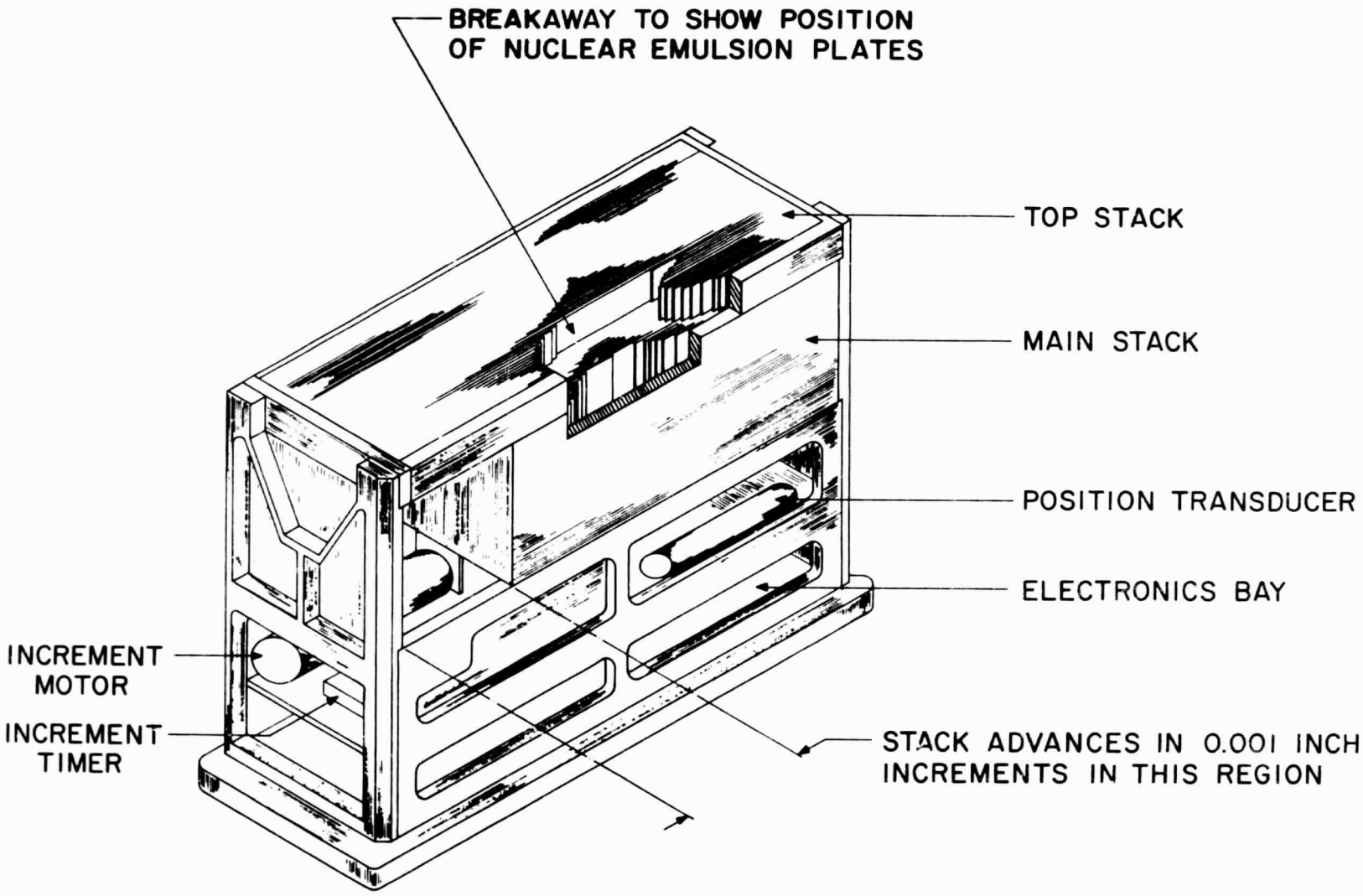

S-9 EXPERIMENT

Fig. 1

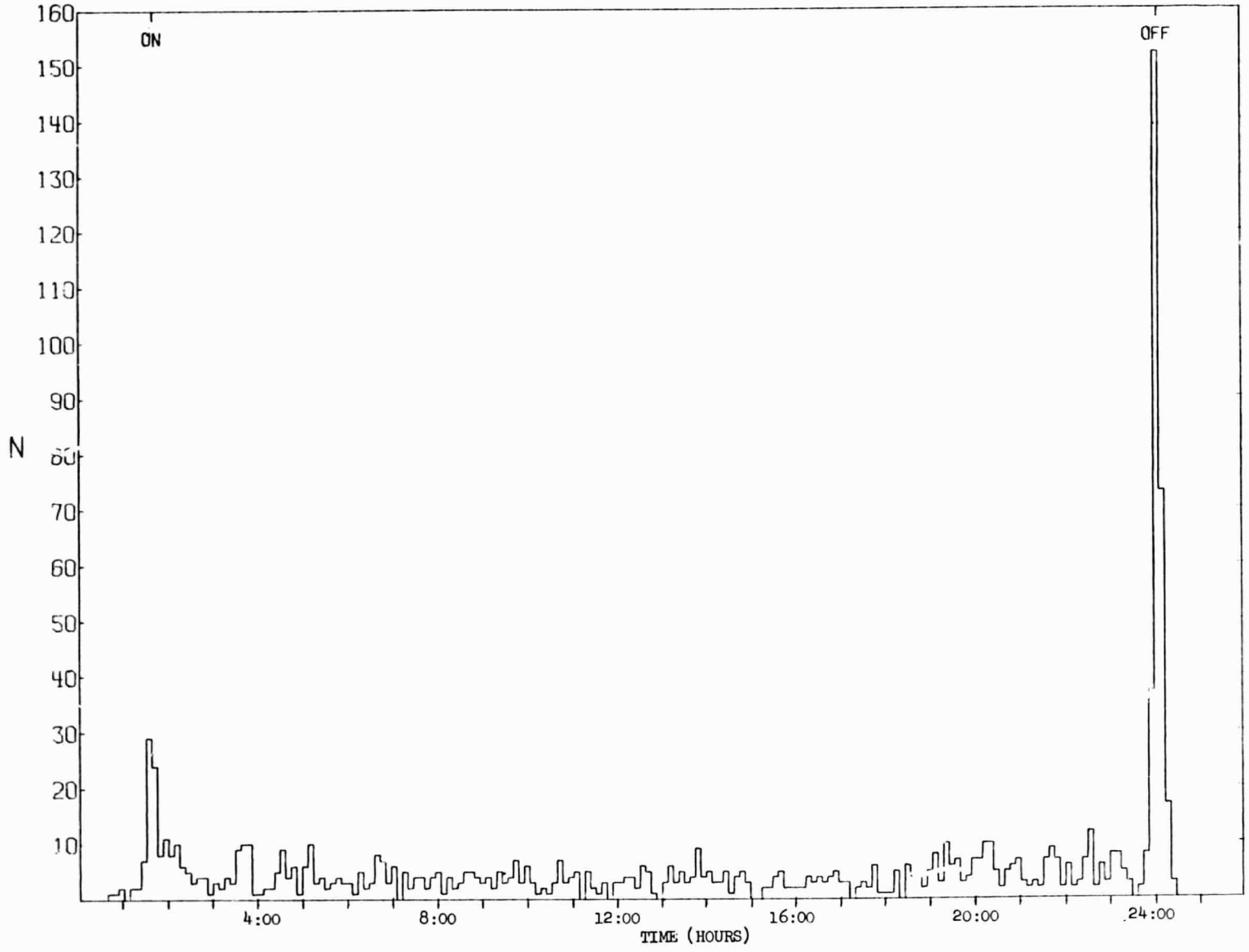
ON
OFF
160
150
140
130
120
110
100
90
80
70
60
50
40
30
20
10
N
4:00
8:00
12:00
16:00
20:00
24:00
TIME (HOURS)

Fig. 2

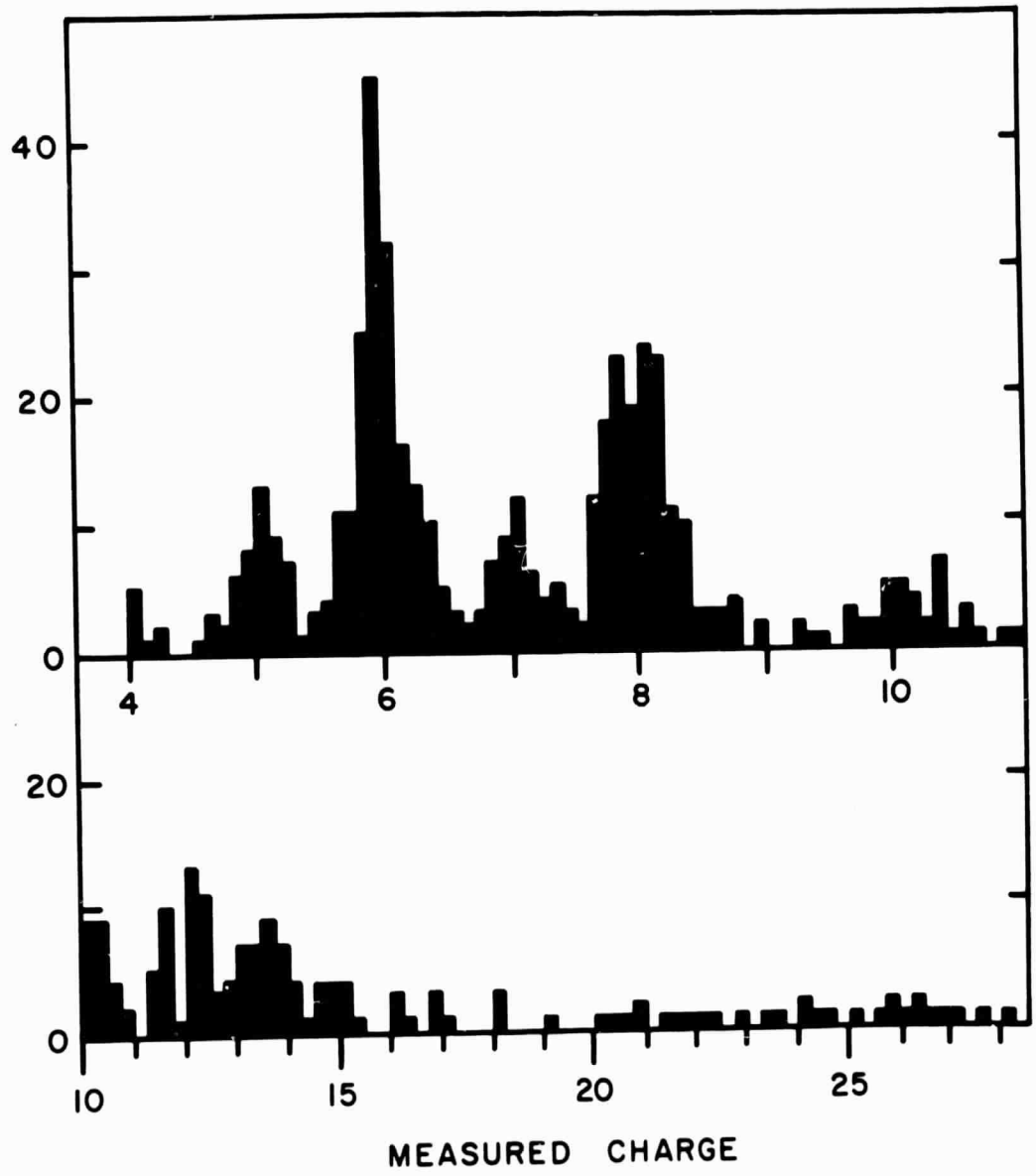

Fig. 3

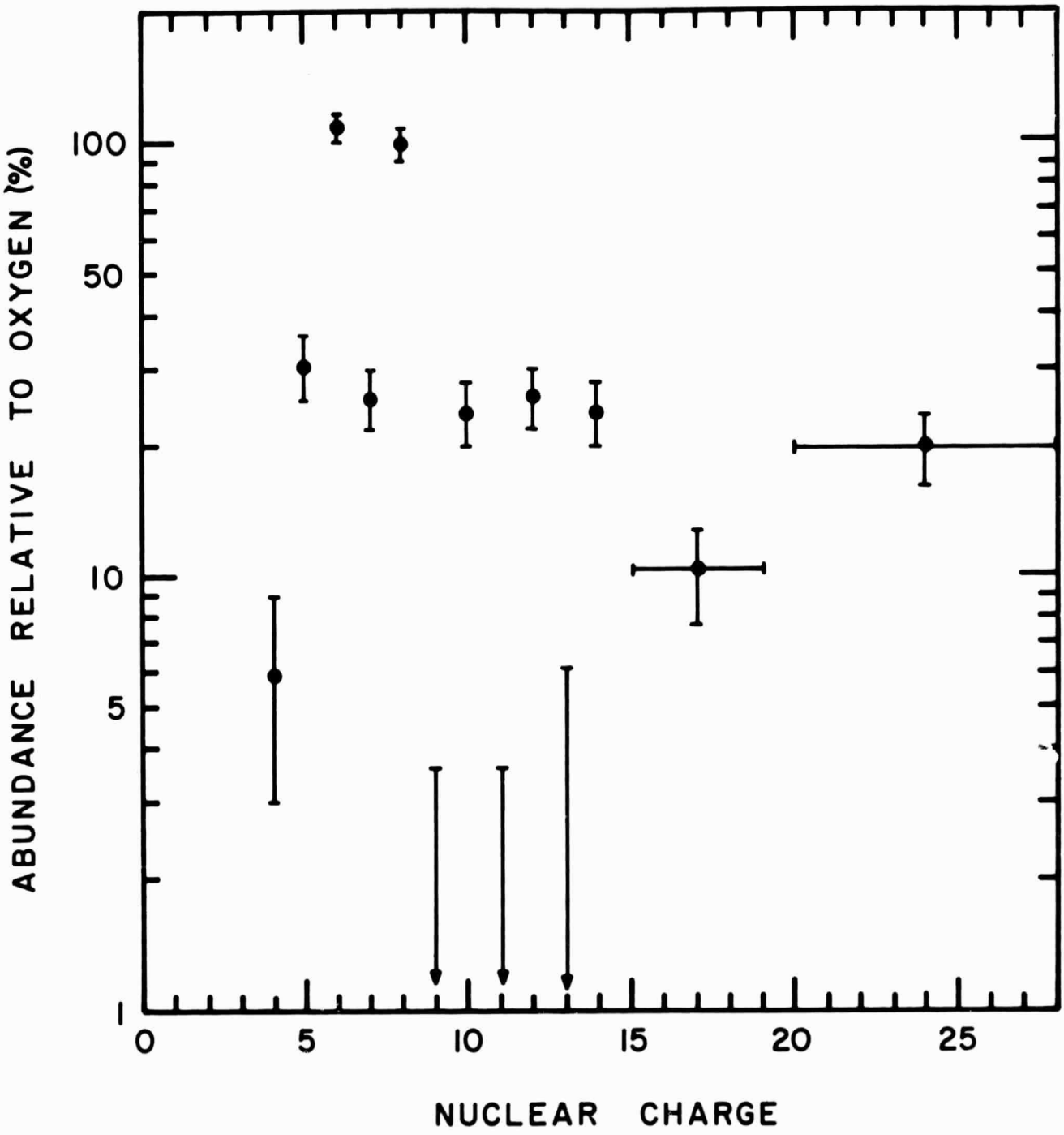
ABUNDANCE RELATIVE TO OXYGEN (%)
100
50
10
5
1
0
5
10
15
20
25
NUCLEAR CHARGE

Fig. 4